Carcinogenesis, 2019, Vol. 40, No. 8, 998–1009

doi:10.1093/carcin/bgy192
Advance Access publication December 27, 2018
Original Article

ORIGINAL ARTICLE

Lapatinib-induced annexin A6 upregulation as an adaptive response of triple-negative breast cancer cells to EGFR tyrosine kinase inhibitors

Sarrah E.Widatalla, Olga Y.Korolkova, Diva S.Whalen, J.Shawn Goodwin, Kevin P.Williams[1], Josiah Ochieng and Amos M.Sakwe*

Department of Biochemistry, Cancer Biology, Neuroscience and Pharmacology, School of Graduate Studies and Research, Meharry Medical College, Nashville, TN 37208, USA and [1]Department of Pharmaceutical Sciences and BRITE Institute, North Carolina Central University, 1005 Dr. DB Todd Jr. Blvd, Durham, NC 27701, USA

*To whom correspondence should be addressed. Tel: +1 615 327 6064; Fax: +1 615 327 6442; Email: asakwe@mmc.edu

Abstract

The epidermal growth factor receptor (EGFR) is a major oncogene in triple-negative breast cancer (TNBC), but the use of EGFR-targeted tyrosine kinase inhibitors (TKI) and therapeutic monoclonal antibodies is associated with poor response and acquired resistance. Understanding the basis for the acquired resistance to these drugs and identifying biomarkers to monitor the ensuing resistance remain a major challenge. We previously showed that reduced expression of annexin A6 (AnxA6), a calcium-dependent membrane-binding tumor suppressor, not only promoted the internalization and degradation of activated EGFR but also sensitized TNBC cells to EGFR-TKIs. Here, we demonstrate that prolong (>3 days) treatment of AnxA6-low TNBC cells with lapatinib led to AnxA6 upregulation and accumulation of cholesterol in late endosomes. Basal extracellular signal-regulated kinase 1 and 2 (ERK1/2) activation was EGFR independent and significantly higher in lapatinib-resistant MDA-MB-468 (LAP-R) cells. These cells were more sensitive to cholesterol depletion than untreated control cells. Inhibition of lapatinib-induced upregulation of AnxA6 by RNA interference (A6sh) or withdrawal lapatinib from LAP-R cells not only reversed the accumulation of cholesterol in late endosomes but also led to enrichment of plasma membranes with cholesterol, restored EGFR-dependent activation of ERK1/2 and sensitized the cells to lapatinib. These data suggest that lapatinib-induced AnxA6 expression and accumulation of cholesterol in late endosomes constitute an adaptive mechanism for EGFR-expressing TNBC cells to overcome prolong treatment with EGFR-targeted TKIs and can be exploited as an option to inhibit and/or monitor the frequently observed acquired resistance to these drugs.

Introduction

Triple-negative breast cancer (TNBC) is mostly diagnosed as high-grade tumors with poor prognosis (1,2). Although TNBCs lack estrogen and progesterone receptors (ER, PR) as well as human epidermal growth factor receptor 2 (HER2), ~60–80% of these tumors are epidermal growth factor receptor (3) positive (4–6). Consequently, epidermal growth factor receptor (EGFR) has not only been an attractive therapeutic target in these tumors but has indeed been targeted with therapeutic monoclonal antibodies such as cetuximab (Erbitux) (7,8) and with tyrosine kinase inhibitors (TKIs) such as lapatinib (9,10). Although these drugs are known to efficiently inhibit EGFR function, their use in TNBC patients is associated with modest or poor efficacies and in particular, relatively rapid relapse of more aggressive tumors due to emergence of resistance (11,12). The acquired resistance to EGFR-TKIs is partly attributed to the activation of other receptor tyrosine kinases (RTKs) including

Received: October 26, 2018; **Revised:** December 19, 2018; **Accepted:** December 27, 2018

Abbreviations

ACTB	β actin
AnxA6	annexin A6
EGFR	epidermal growth factor receptor
ERK1/2	extracellular signal-regulated kinase 1 and 2
HER2	human epidermal growth factor receptor 2
LAP-R	lapatinib-resistant cells
LAP-R-A6sh5	AnxA6 targeting shRNA transfected lapatinib-resistant cells
LAP-R-NSC	non-silencing control shRNA transfected lapatinib-resistant cells
PAR	parental cells
PBS	phosphate-buffered saline
RTKs	receptor tyrosine kinases
shRNAs	small-hairpin RNAs
SOCE	store-operated Ca^{2+} entry
TKIs	tyrosine kinase inhibitors
TNBC	triple-negative breast cancer

c-MET (13) as well as the Ras/MAP kinase (14) and other downstream signaling pathways. Unfortunately, inhibition of EGFR in combination with other RTKs sensitizes cells to these drugs but does not prevent the development of resistance to TKIs.

Cholesterol- and sphingolipid-rich membrane microdomains or lipid rafts besides their role in the clustering of oncogenic receptors (15–17) including EGFR not only serve as efficient platforms for oncogenic cellular signaling (18,19), but have also been implicated in acquired resistance to TKIs. Therefore, lipid raft-rich breast and prostate cancer cell lines were reported to be more sensitive to cholesterol depletion than their counterparts with normal lipid raft content (20,21). Also, localization of EGFR in lipid rafts has been shown to be associated with resistance of BC cells to gefitinib and that statin-mediated reduction in cholesterol in lipid rafts sensitized the cells to the TKI (15). Although cholesterol represents a major constituent of lipid rafts (22), many other protein families are localized to and affect the functional integrity of these membrane microdomains. Some members of the annexin family of Ca^{2+}-dependent membrane binding proteins, such as annexin A6 (AnxA6), have been shown to not only co-localize with cholesterol at the plasma membrane, but also undergo similar trafficking and subcellular localization throughout the endocytic pathway (23). Besides its tumor suppressor functions (24), we have also shown that downregulation or loss of AnxA6 in TNBC cells is associated with rapid degradation of raft-associated receptors such as activated EGFR, and sensitization of the cells to EGFR-TKIs (25). However, the involvement of AnxA6 in acquired resistance to EGFR/HER2-TKIs remains poorly understood.

In the present study, we demonstrate that prolonged treatment of the potentially more aggressive AnxA6-low TNBC cells with EGFR/HER2-TKIs, but not cytotoxic drugs such as carboplatin or paclitaxel, led to AnxA6 upregulation and accumulation of cholesterol in late endosomes. These novel lapatinib-induced effects were reversed following lapatinib withdrawal or by RNAi-mediated inhibition of lapatinib-induced expression of AnxA6. Our data suggest that induction of AnxA6 and accumulation of cholesterol in late endosomes by lapatinib not only constitutes a novel mechanism for the development of resistance to EGFR-TKIs but can also be exploited to attenuate and/or monitor acquired resistance to these drugs.

Materials and methods

Cell lines and cell culture

MDA-MB-468 and HCC70 basal-like breast cancer cell lines were purchased from American Type Culture Collection (ATCC). Cells were expanded, cryopreserved at –80°C and only early passages (< passage 5) of these cell lines were used in the experiments described in this manuscript. Prophylactic mycoplasma treatment of the cells was also routinely carried out on recovery of the cell stocks. These cell lines were authenticated by analysis of 15 autosomal short tandem repeat loci on 23 and 24 October 2018 (Genetica Cell Line Testing, Burlington, NC). The HCC70 cell line was cultured in DMEM/F12 containing 10% fetal bovine serum and Pen/Strep (100 units/ml penicillin and 50 units/ml streptomycin). MDA-MB-468 cells were maintained in medium L-15 (Leibovitz) containing 10% fetal bovine serum, Pen/Strep and 0.15% sodium bicarbonate. Cells were maintained at 37°C in a humidified CO_2 incubator. Where indicated, serum-starvation of cells was achieved by culturing the cells in their respective media containing 0.5% fetal bovine serum for 12–16 h. For transient treatment of cells with drugs, the cells were seeded in six-well plates and allowed to attach overnight in complete medium. The medium was aspirated and replaced with fresh medium containing the indicated concentrations of the indicated drugs. Drug-containing media were replaced every 2–3 days.

Antibodies and other reagents

Antibodies against EGFR, phospho-EGFR (pY1068), phospho-extracellular signal-regulated kinase 1/2 (pERK1/2, T202/Y204) and ERK1/2 were purchased from Cell Signaling Technology (Beverly, MA). Antibodies against AnxA6 and LAMP-1 as well as secondary anti-mouse, anti-goat and anti-rabbit horseradish peroxidase-conjugated antibodies were purchased from Santa Cruz Biotechnology (Dallas, TX). Filipin and antibodies against β-actin (ACTB) were purchased from Sigma (St. Louis, MO). A set of EGFR-TKIs including lapatinib ditosylate, erlotinib, gefitinib and canertinib as well as Paclitaxel and Carboplatin were purchased from BioVision (Milpitas, CA). Except otherwise indicated, all other reagents were purchased from Sigma and Life Technologies.

Generation of lapatinib-resistant MDA-MB-468 cells

Early passage MDA-MB-468 cells were seeded in 10-cm dishes and maintained in Leibovitz's L15 medium supplemented as above at 37°C in a humidified CO_2 incubator. The cells were treated with 2 μM lapatinib with changes in medium every 2–3 days for up to 4 months. During this treatment, cells were passaged when they were ~80% confluent. About 10% of the cells were seeded for continuous treatment while the remaining cells were cryopreserved and also stored as cell pellets at –80°C. The passages were denoted P1–P4, respectively, and are herein referred to as lapatinib-resistant MDA-MB-468 (LAP-R) cells. For additional experiments, P3 were used as LAP-R cells.

Plasmid constructs and transfections

Small-hairpin RNAs (shRNAs) targeting the coding sequence of AnxA6 (A6sh) in pGIPZ lentiviral vector, a non-silencing shRNA control (26) (GE Dharmacon), were used to prepare lentiviral stocks in 293 T cells, and the viral particles were used to infect LAP-R (P3) breast cancer cells as described previously (25). The resulting subclones of LAP-R cells were denoted LAP-R-NSC, LAP-R-A6sh5 and LAP-R-A6sh2. Downregulation of AnxA6 was verified by immunoblotting.

Immunofluorescence microscopy

Cells were plated sparsely on glass cover slips and allowed to grow until they formed visible colonies. Indirect immunofluorescence staining was performed as described previously (5) using antibodies to EGFR, AnxA6 or LAMP-1. Images were captured using a Nikon A1R confocal microscope with 60× or 40× oil immersion objectives and analyzed using the NIS software. Subcellular localization and/or distribution of cholesterol was detected by staining the cells with filipin (Sigma, F9765). The stained cells were mounted with EverBrite™ Mounting Medium without 4′,6-diamidino-2-phenylindole (Biotium # 23001) and visualized using a wide field confocal microscope as described previously (27). For co-localization of cholesterol and either LAMP-1, AnxA6 or EGFR, cells were fixed in 4% paraformaldehyde at room temperature for 30 min and

then stained with the respective primary antibodies followed by the conjugated secondary antibodies. The cells were then washed thoroughly in phosphate-buffered saline (PBS) and stained with filipin (12.5 µg/ml) for 1 h at room temperature in the dark. The double-stained cells were then rinsed in PBS and mounted as described earlier.

Density gradient centrifugation

Cells were grown to 70–80% confluency in 15-cm dishes, washed and scraped in ice-cold Hanks' balanced salt solution (Life Technology). The cell pellet was resuspended in base buffer (20 mM Tris–HCl, pH 7.8, 250 mM sucrose) containing 1 mM $CaCl_2$, 1 mM $MgCl_2$, protease inhibitor cocktail (Sigma) and phosphatase inhibitors (20 mM sodium fluoride, 1 µm sodium orthovanadate and 50 mM beta-glycerophosphate). Cells were lysed by Dounce homogenization and by passing the homogenate through a 27G needle. The homogenate was centrifuged at 2300*g* for 4 min at 4 C, and the post-nuclear supernatant was separated by density gradient centrifugation as described previously (28) using a continuous Optiprep gradient (5–30%) in base buffer. The gradients were centrifuged at 35 000 rpm (SW-41 rotor) and at 4°C for 2.5 h. Gradients were then fractionated from the top, and the sedimentation of the indicated proteins was assessed by western blotting.

Western blotting

BC cells were cultured until they were 70% confluent, then serum-starved overnight and treated with or without 50 ng/ml EGF (EMD Biosciences) in Hanks' balanced salt solution containing 1 mM Ca^{2+} and 1 mM $MgCl_2$ for the indicated time periods. The EGF-treated cells were scraped in ice-cold Hanks' balanced salt solution and whole-cell lysates prepared in radio-immunoprecipitation (RIPA) buffer as described previously (5). EGFR activation was detected by immunoblotting with anti-EGFR (pY1068) and antibodies to total EGFR. Activation of downstream signaling cascades was assessed by western blotting using anti-pERK1/2 (pT202/pY204). Immunoblotting with antibodies against ERK1/2 and/or ACTB was used as the loading controls. Immune complexes were revealed by enhanced chemiluminescence, scanned and quantified using NIH Image J software.

Cholesterol measurements

Cholesterol in the gradient fractions was determined by using equal volumes of the gradient fractions and the Amplex™ Red Cholesterol Assay Kit (Life Technologies) according to the manufacturer's instructions. For determination of total cellular cholesterol, cells were trypsinized and equal number of cells was lysed in an equal volume of RIPA buffer without protease or phosphatase inhibitors. Equal volumes of cells lysate were then used to determine cholesterol concentration using the Amplex™ Red cholesterol assay kit. Results were normalized to total cellular protein.

Cell proliferation assays and clonogenic assays

Cells were seeded in 24-well plates in triplicates using 1×10^4 cells/well, as described previously (5). The proliferation and viability of the cells were determined using the PrestoBlue reagent (Invitrogen) diluted in serum-free medium according to the manufacturer's instructions. For clonogenic assays, 5000 cells were seeded in six-well plates and allowed to grow for up to 2 weeks. The viability of the cells was assessed by using the PrestoBlue reagent followed by fixation in 3.7% formaldehyde in PBS and staining with crystal violet as described previously (29).

RNA isolation and real-time PCR

Total RNA was extracted from cells using the RNeasy Mini Kit (QIAGEN). Equal amounts of total RNA were used for cDNA synthesis using the iScript cDNA synthesis kit according to the manufacturer's instructions (Bio-Rad), and real-time PCR was performed as described previously (30) using ANXA6 and ACTB Taqman gene-specific assays and universal PCR master mix (Life Technologies).

Results

Treatment of TNBC cells with EGFR-TKIs but not cytotoxic drugs induces AnxA6 expression

We previously reported that downregulation of AnxA6 in TNBC cell lines not only led to rapid internalization of activated EGFR but also sensitized the cells to EGFR/HER2-TKIs (25). In our quest to determine whether AnxA6 is important in the response of TNBC cells to cytotoxic and/or EGFR-targeted therapies, we analyzed changes in the expression of AnxA6 mRNA in clinical samples from the TBCRC001 clinical trial of stage IV TNBC patients before (pre) and after (post) treatment with cetuximab with or without carboplatin (7). This analysis revealed that treatment of stage IV TNBC tumors ($n = 18$) with cetuximab/carboplatin was associated with AnxA6 upregulation ($P = 0.039$, Wilcoxon signed rank test), and more specifically, AnxA6 was upregulated in 77.8% (14/18) of the samples (Figure 1A). To determine whether the upregulation of AnxA6 in the post-treatment clinical samples was due to EGFR inhibition or the chemotherapeutic drug, we examined whether treatment of TNBC cells with EGFR-TKIs and cytotoxic drugs led to altered cellular levels of AnxA6. We show that treatment of MDA-MB-468 and HCC70 cells with lapatinib led to AnxA6 upregulation by day 3 (Figure 1B). Although the extent of lapatinib-induced expression of AnxA6 was EGFR-TKI and cell-type dependent, we show that treatment of MDA-MB-468 cells with various concentrations of gefitinib, erlotinib and canertinib also led to AnxA6 upregulation (Figure 1C). On the contrary, treatment of MDA-MB-468 cells with paclitaxel (Figure 1D) or carboplatin (Figure 1E) had no effect on the cellular levels of AnxA6. The 2 µM concentration of lapatinib used in this study is consistent with its maximum plasma concentration when used at 900–1600 mg of single doses (31). Likewise, the dose ranges of Paclitaxel and Carboplatin are consistent with the maximum plasma concentrations of these drugs when used respectively at 40–80 and 375 mg/m^2 (32,33). Together, this suggests that unlike treatment with cytotoxic chemotherapeutic drugs, treatment of TNBC cells with EGFR-TKIs is accompanied by upregulation of AnxA6 and underscores the distinct mechanisms of resistance to chemotherapeutic and EGFR-targeted treatment regimens.

AnxA6 upregulation is associated with accumulation of cholesterol in lapatinib-treated TNBC cells

It is well established that treatment of TNBC cells with EGFR/HER2-TKIs is associated with resistance to the drugs (34) and that upregulation of AnxA6 is associated with decreased cell growth (35). To further characterize the contribution of AnxA6 on acquired resistance of TNBC cells to EGFR-TKIs, MDA-MB-468 cells with amplified levels of EGFR and lapatinib treatment were used in subsequent investigations. We first showed that treatment of asynchronously growing MDA-MB-468 cells with lapatinib effectively inhibited (>90% by day 2) the activation of EGFR (Figure 2A) and that treatment of these cells with lapatinib attenuated their growth by ~30% within 72 h (Figure 2B). We then established LAP-R cells as described in Materials and methods. Compared with the parental (PAR) control cells, AnxA6 was upregulated by >3-fold in P1 and >5-fold in P4 LAP-R cells (Figure 2C and D). Isolation of total RNA from control and LAP-R cells and assessment of AnxA6 mRNA expression by RT–PCR revealed that lapatinib-induced expression of AnxA6 occurred at the mRNA level (Figure 2E). Using clonogenic assays (Figure 2F) followed by assessment of cell viability (Figure 2G), we show that the LAP-R cells were indeed resistant to lapatinib treatment (2 µM) compared with PAR cells.

Based on previous reports showing that cholesterol is dysregulated in cancer (36) and that AnxA6 influences the distribution of cholesterol in most cell types (23), we speculated that lapatinib-induced expression of AnxA6 would affect the distribution of cholesterol in lapatinib-treated cells. To accomplish this, PAR and LAP-R cells were stained with

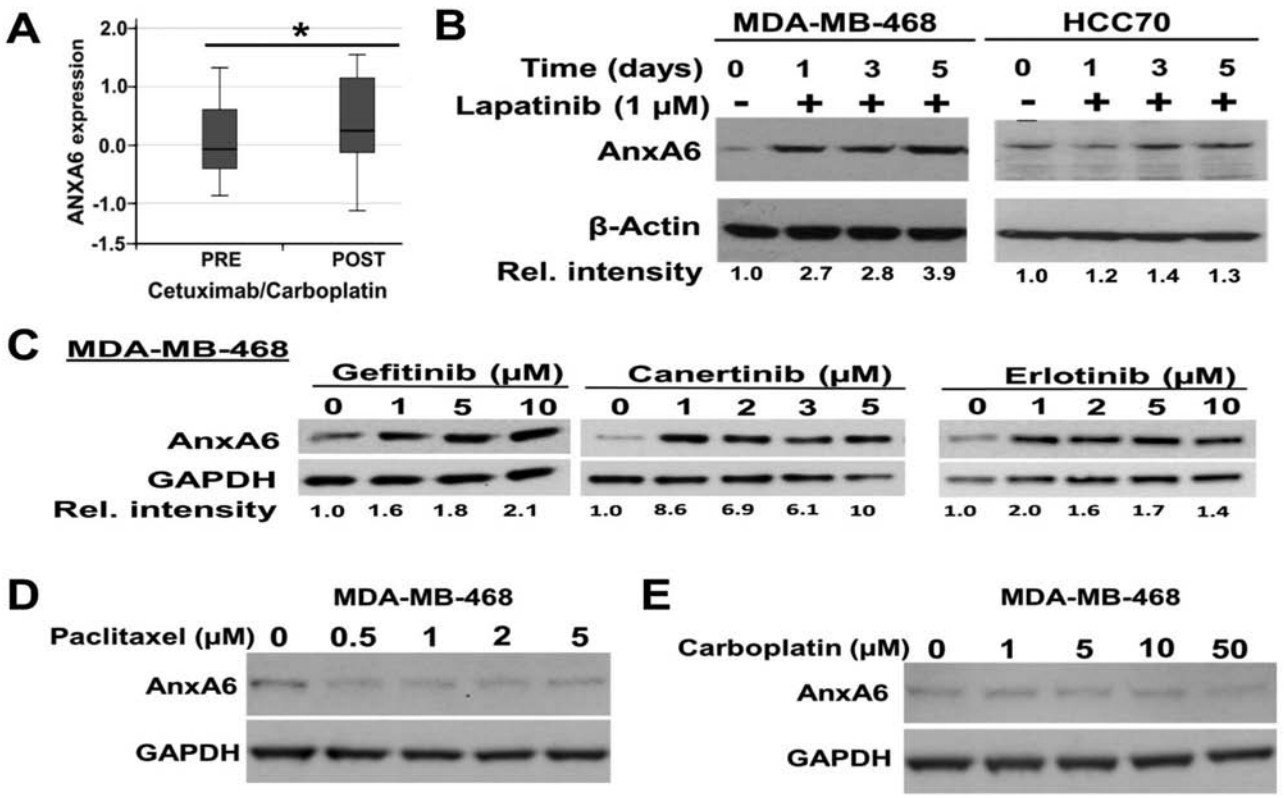

Figure 1. Lapatinib induces AnxA6 expression in TNBC cells. (**A**) AnxA6 mRNA levels from a microarray analysis of tissues from TBCRC001 clinical trial of stage IV TNBC patients before (pre) and after (post) treatment with cetuximab with or without carboplatin. *AnxA6 expression in pretreatment versus post-treatment tissues ($P = 0.039$). (**B–E**) Representative blots of the effects of lapatinib on the expression of AnxA6. The indicated cell lines were treated with 1 μM lapatinib for up to 5 days (B), the indicated concentrations of gefitinib, canertinib and erlotinib (C) or the cytotoxic drugs paclitaxel (D) or carboplatin (E). Equal amounts of whole-cell extracts were analyzed by western blotting using antibodies against AnxA6 and GAPDH as the loading control. The relative intensity of the protein bands was analyzed using the NIH Image J software and quantified relative to control mock-treated cells.

filipin, a naturally fluorescent polyene antibiotic that binds to cholesterol, and visualized the staining by wide-field microscopy using the ×10 magnification as described previously (27). Filipin staining revealed that cholesterol was associated with the cell periphery in PAR cells (Figure 3A, left panel) but was not only more abundant but also mostly intracellular in the LAP-R cells (Figure 3A, right panel). Co-staining of filipin and LAMP-1 revealed that the predominantly intracellular cholesterol in LAP-R cells co-localized with LAMP-1 but not in PAR cells (Figure 3B). To quantify the effect of lapatinib on whole-cell cholesterol, we show that lapatinib treatment was associated with increased levels (>3-fold) of whole-cell cholesterol in LAP-R cells compared with PAR cells. Maintenance of LAP-R cells in the absence of lapatinib for up to 5 days as depicted in Figure 3C, led to a slight reduction in the total cellular cholesterol in LAP-R cells (Figure 3D). Treatment of PAR and LAP-R cells with methyl-β-cyclodextrin revealed that LAP-R cells were more sensitive to cholesterol sequestration compared with PAR cells (Figure 3E). We also show that withdrawal of lapatinib from the resistant cells for 5 days led to a 2- to 3-fold decrease in AnxA6 protein levels (Figure 3F). Together, this suggests that lapatinib-induced AnxA6 upregulation and accumulation of cholesterol in late endosomes potentially contributes to the acquired resistance to this drug and that the lapatinib-induced upregulation of AnxA6 in TNBC cells is reversible.

Lapatinib-induced expression of AnxA6 affects the distribution of lipid raft markers and cholesterol in TNBC cells

We fractionated post-nuclear supernatants from PAR and LAP-R cells after separation in continuous Optiprep gradients. Analysis of the gradient fractions by western blotting revealed that lipid raft markers (flotillin and EGFR) were concentrated in the lighter fractions 4–5 in LAP-R cells (Figure 4A and B) and in heavier fractions 6–7 in the PAR cells (Figure 4C and D). This analysis also revealed that lapatinib-induced expression of AnxA6 was associated with relatively more lipid raft-associated flotillin and EGFR in LAP-R cells (Figure 4A–D). Detection of Na^+/K^+ ATPase in the gradient fractions was used as a marker for plasma membranes including lipid rafts (37). Although flotillin, EGFR and lapatinib-induced AnxA6 co-migrated with Na^+/K^+ ATPase, these proteins were not restricted to the plasma membrane fractions (Figure 4A and B) and that Na^+/K^+ ATPase is known to be endocytosed in cancer cells (38). Analysis of cholesterol in the gradient fractions revealed that cholesterol levels were significantly higher in LAP-R cells compared with PAR cells and that in LAP-R cells, most of the cholesterol was in fractions 4–6 (Figure 4E), which also contained the highest levels of AnxA6 (Figure 4C and D). Although this suggests that lapatinib-induced AnxA6 and cholesterol are within the same cellular compartment, data from these sedimentation assays appear to contradict the predominant endosomal localization of cholesterol in LAP-R cells depicted in Figure 3A. This may be attributed, in part, to the notion that sedimentation in Optiprep or other gradient

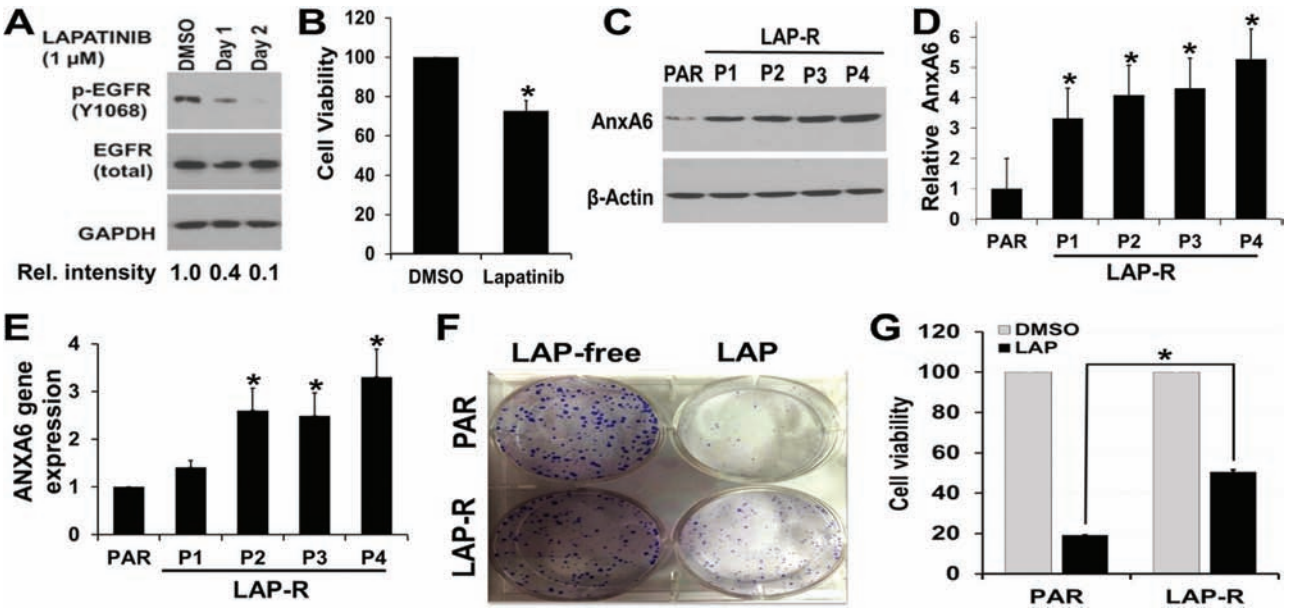

Figure 2. AnxA6 is upregulated in LAP-R cells. (**A**) MDA-MB-468 cells were grown and treated with lapatinib (1 μM) for up to 2 days and processed for western blot using indicated antibodies. (**B**) MDA-MB-468 cells were treated with dimethyl sulfoxide (DMSO) vehicle or lapatinib (1 μM) for 72 h, and the viability of the cells was determined using PrestoBlue cell viability assay reagent. (**C–F**) LAP-R cells were established by continuous treatment of PAR cells with 2 μM lapatinib for up to 4 months. Four passages (P1–P4) were collected and the expression of AnxA6 protein was verified by western blotting (C and D). Changes in AnxA6 mRNA levels were assayed RT–PCR (E), and the effect of lapatinib (2 μM) treatment on the growth and viability of the LAP-R cells (P3) was verified by clonogenic assays (F) and PrestoBlue cell viability assays (**G**). Experiments were repeated at least three times. *Significant ($P < 0.05$) increase in AnxA6 protein or mRNA levels (D and E, respectively) or the viability of lapatinib-treated PAR versus LAP-R cells (G).

materials does not effectively separate plasma membranes from endosomal membranes. It has also been shown that in response to a decrease in plasma membrane cholesterol or cellular transformation, Na^+/K^+ ATPase, known to be an integral plasma membrane protein, is frequently endocytosed and becomes localized in late endosomes (38). It is, therefore, possible that the gradient fractions with the highest cholesterol also contained endosomal membranes. We next show by immunofluorescence that the total cellular levels of lapatinib-induced AnxA6 in LAP-R cells changed from essentially endosomal to plasma membranes following the withdrawal of lapatinib from LAP-R cells (Figure 4F), and this consistent with the reduced overall levels of AnxA6 as depicted in Figure 3F.

Upregulation of AnxA6 is critical for acquired resistance to lapatinib in TNBC cells

To demonstrate that lapatinib-induced AnxA6 expression is required for acquired resistance to lapatinib, we used RNAi technology to block the lapatinib-induced upregulation of AnxA6 in LAP-R cells. To do this, we stably transfected LAP-R cells with lentiviruses expressing a non-silencing control (26) shRNA and two shRNAs, herein denoted A6sh2 and A6sh5, targeting distinct regions of the coding sequence of AnxA6. Treatment of the transfected cells with lapatinib and analysis of AnxA6 expression revealed that lapatinib-induced AnxA6 expression was blocked by ~60% in LAP-R-A6sh2 cells and >80% in LAP-R-A6sh5 cells compared with LAP-R-NSC control cells (Figure 5A and B).

We next cultured PAR and LAP-R cells as well as LAP-R-NSC and LAP-R-A6sh5 cells in the presence or absence of lapatinib as in Figure 3C and either examined filipin staining by widefield microscopy (Figure 5C and D) or filipin and LAMP-1 staining by confocal microscopy (Figure 5E and F). Filipin staining of the cells revealed that continuous treatment of LAP-R cells with lapatinib led to the accumulation of cholesterol in late endosomes (Figure 5C, upper panel and Figure 5E, left panel). On the contrary, and consistent with data in Figure 3B, inhibition of AnxA6 upregulation in LAP-R-A6sh5 cells blocked the accumulation of cholesterol in late endosomes and that most of the cholesterol was associated with the plasma membrane (Figure 5D, upper panel and Figure 5F, left panel). Following withdrawal of lapatinib from lapatinib-treated cells, and consistent with the decrease in AnxA6 expression levels (Figure 3F), whole cellular cholesterol levels were similar to that in untreated PAR cells and the filipin staining was restricted to the plasma membrane. In the confocal images as opposed to the widefield images, inhibition of AnxA6 upregulation by RNA interference led to diffuse distribution of cholesterol upon removal of lapatinib (Figure 5C and D, lower panels and Figures 5E and F, right panels). Together, this suggests that the accumulation of cholesterol in TNBC cells requires continuous treatment with lapatinib and lapatinib-induced expression of AnxA6.

We next assessed whether blocking lapatinib-induced AnxA6 expression affected the viability of TNBC cells with or without lapatinib treatment. To do this, PAR, LAP-R as well as LAP-R-NSC and LAP-R-A6sh5 cells were grown in the presence and absence of lapatinib as depicted in Figure 3C followed by cell viability assays. Consistent with data in Figure 2F and G, cell growth and viability assays revealed that PAR cells were more sensitive to lapatinib than LAP-R cells and that in the presence of lapatinib, LAP-R-A6sh5 cells showed >1.5-fold sensitivity to lapatinib treatment compared with LAP-R-NSC control cells (Figure 5G). Upon withdrawal of lapatinib, there was no noticeable difference in the growth of PAR and LAP-R cells. However, withdrawal of lapatinib was associated with increased growth of LAP-R-A6sh5 cells (Figure 5H), consistent

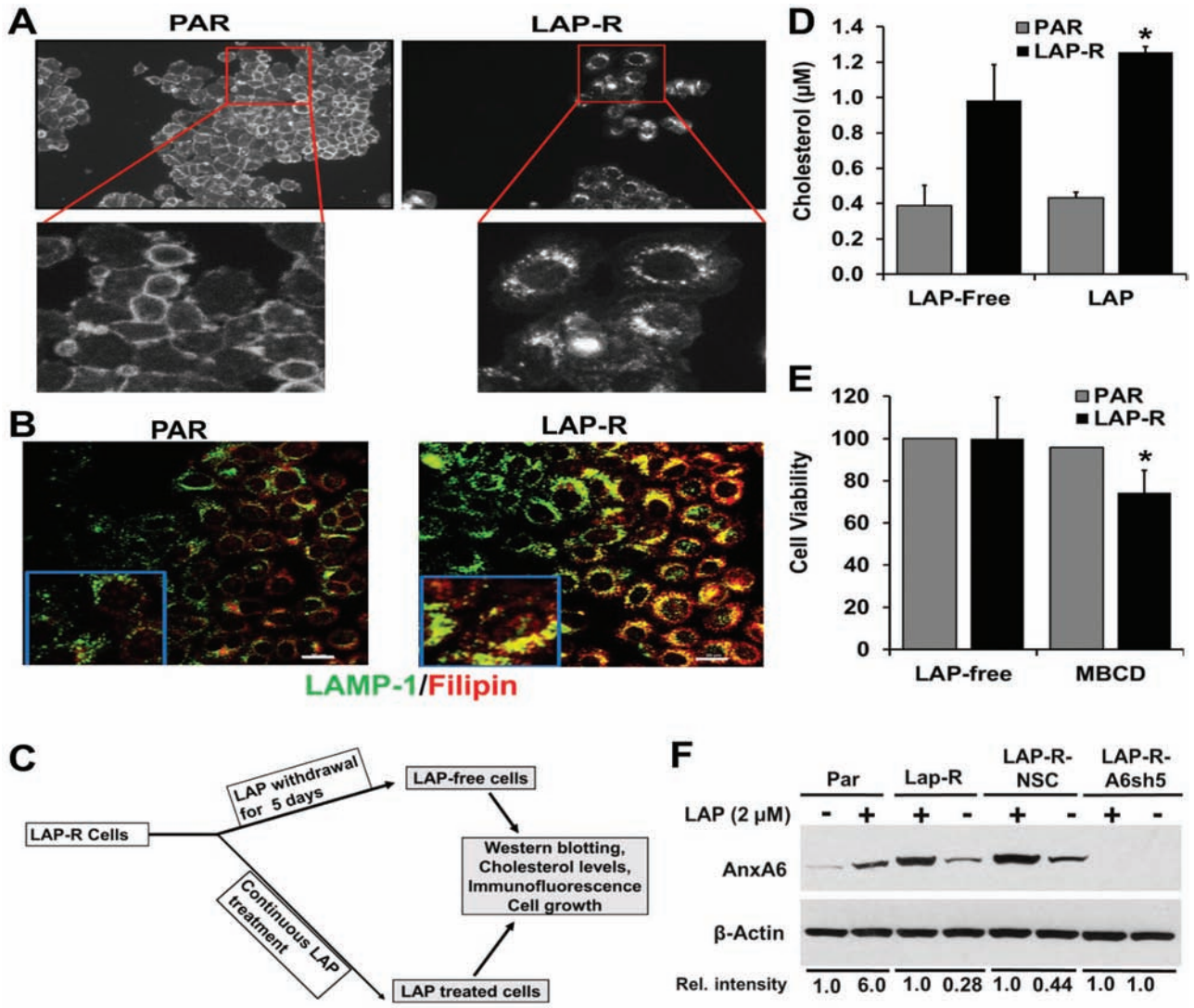

Figure 3. Prolong treatment of MDA-MB-468 cells with lapatinib lead to accumulation of cholesterol in late endosomes. (**A**) Parental (PAR) cells in complete medium and LAP-R cells in lapatinib-supplemented medium were grown in glass coverslips. Cells were rinsed in PBS, fixed in 4% paraformaldehyde, washed and incubated with filipin for 1 h. (**B**) Cells were prepared as described earlier, incubated with rabbit antibodies against LAMP-1 followed by FITC-conjugated anti-rabbit and then processed for detection of cholesterol by incubation with filipin as described earlier. Cellular localization of cholesterol (filipin staining) and LAMP-1 were visualized by wide field (A) and confocal (B) microscopy, respectively. White bars indicate 20 μm. (**C**) Schematic representation of lapatinib withdrawal from LAP-R cells. LAP-R cells were either continuously grown in lapatinib (2 μM) containing complete medium or maintained in the same medium without lapatinib for 5 days (LAP free) before use in experiments. (**D**) Effect of lapatinib on total cellular cholesterol. Equal numbers of PAR or LAP-R cells were grown in the presence or absence of lapatinib, harvested and lysed in RIPA buffer. Total cellular cholesterol was determined using the Amplex Red Cholesterol Assay. (**E**) Sensitivity of LAP-R cells to cholesterol sequestration. Equal number of cells were grown and treated with methyl-β-cyclodextrin (0.4 mM) for 5 days, and cell viability was determined as in Figure 2F. *$P < 0.05$. (**F**) Withdrawal of lapatinib treatment of TNBC cells restores AnxA6 expression to basal levels. The indicated cell lines were treated with lapatinib as in (C). Cells were harvested and equal amounts of whole-cell extracts were used to determine the expression of AnxA6 protein by western blotting. Detection of ACTB was used as the loading control. The relative intensity of AnxA6 expression in a representative experiment is indicated relative to untreated versus lapatinib-treated PAR cells or in continuous lapatinib treatment versus lapatinib-free medium for LAP-R cells.

with the tumor suppressor function of AnxA6 (25). Together with data in Figure 3, this suggests that lapatinib-induced expression of AnxA6 and accumulation of cholesterol in late endosomes are critical for acquired resistance of TNBC cells to EGFR-TKIs.

Withdrawal of lapatinib treatment leads to loss of cholesterol from late endosomes and enrichment of plasma membranes with cholesterol

Figure 3 revealed that a proportion of the predominantly late endosomal cholesterol in LAP-R cells was lost following in vitro culture of the cells in the absence of lapatinib. To determine the fate of lapatinib-induced cholesterol upon withdrawal of lapatinib, LAP-R cells were cultured in the presence or absence of lapatinib and then co-stained with filipin and LAMP-1. Filipin and LAMP-1 staining revealed that withdrawal of lapatinib was accompanied by both diminished levels of cholesterol, loss of co-localization of filipin with LAMP-1 and a conspicuous filipin staining in the plasma membrane (Figure 6A, arrow heads). Quantitative analysis of the co-localization of LAMP-1 and filipin in the plasma membrane (cell periphery) and late endosomes (intracellular) revealed that withdrawal of lapatinib (LAP free) was associated with loss of co-localization of filipin and LAMP-1 in late endosomes (Figure 6B). To

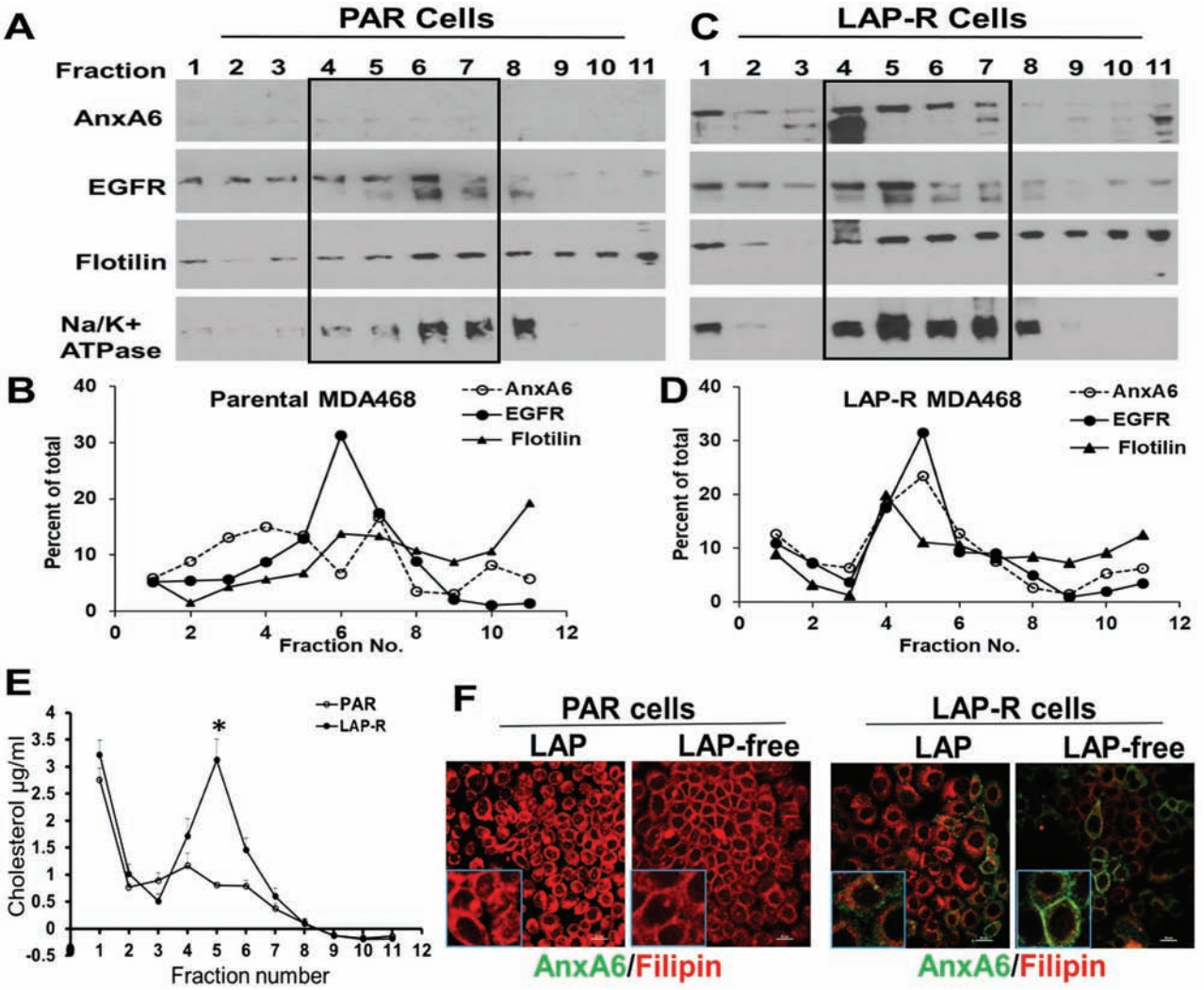

Figure 4. Lapatinib-induced expression of AnxA6 is associated with cholesterol-rich membrane lipid rafts. (**A** and **C**) Post-nuclear supernatants (PNS) from PAR and LAP-R cells were separated by density gradient centrifugation in a continuous Optiprep gradient, and the gradient fractions were analyzed by western blotting using antibodies to the indicated proteins. (**B** and **D**) Densitometric analysis of the separated proteins from a representative experiment. (**E**) Cholesterol in each gradient fraction was determined by the Amplex Red assay. (**F**) Detection of AnxA6 and cholesterol by immunofluorescence. Parental and LAP-R cells were seeded on glass coverslips and maintained in lapatinib containing medium or without lapatinib as depicted in Figure 3C. Cells were stained with antibodies against AnxA6 followed by staining with filipin.

demonstrate that some of the cholesterol was redistributed to the plasma membranes, we co-stained EGFR and filipin in PAR and LAP-R cells. This revealed that in the presence of lapatinib, most of the filipin staining was intracellular (Figure 6C, left panels), and that following withdrawal of lapatinib, filipin co-localized with EGFR at the plasma membrane (Figure 6C, right panels). Quantitative analysis of the co-localization of EGFR and filipin also confirmed that withdrawal of lapatinib (LAP free) was associated with loss of cholesterol in late endosomes and enrichment of the plasma membrane with cholesterol (Figure 6D).

Withdrawal of lapatinib from LAP-R cells reverts the cells from EGFR-independent to EGFR-dependent activation of the MAP kinase pathway

Because MDA-MB-468 cells express amplified levels of EGFR, we speculated that removal of lapatinib from LAP-R cells and the associated enrichment of plasma membranes with cholesterol may revert the cells from EGFR-independent to EGFR-dependent growth. To test this, LAP-R cells were either maintained in lapatinib continuously or cultured in the absence of lapatinib as in Figure 3C. The cells were then serum starved with or without lapatinib, stimulated with EGF and the activation of ERK1/2 assessed by western blotting. As expected, continuous treatment of LAP-R cells with lapatinib strongly inhibited the activation of EGFR while withdrawal of lapatinib restored at least, in part, the activation of the receptor (Figure 6E and F). Even though EGFR was strongly inhibited in LAP-R cells, this was associated with a strong (>3-fold) basal activation of ERK1/2 (Figure 6E and G) and an equally strong (~3-fold) EGF-stimulated ERK1/2 activation. On the other hand, withdrawal of lapatinib (LAP free) was associated with >5-fold EGF-stimulated activation of MAP kinase ERK1/2 (Figure 6E–G). Together with data in Figure 5, this suggests that in LAP-R cells, lapatinib-induced AnxA6 expression and accumulation of cholesterol in late endosomes is associated with EGFR-independent activation of the MAP

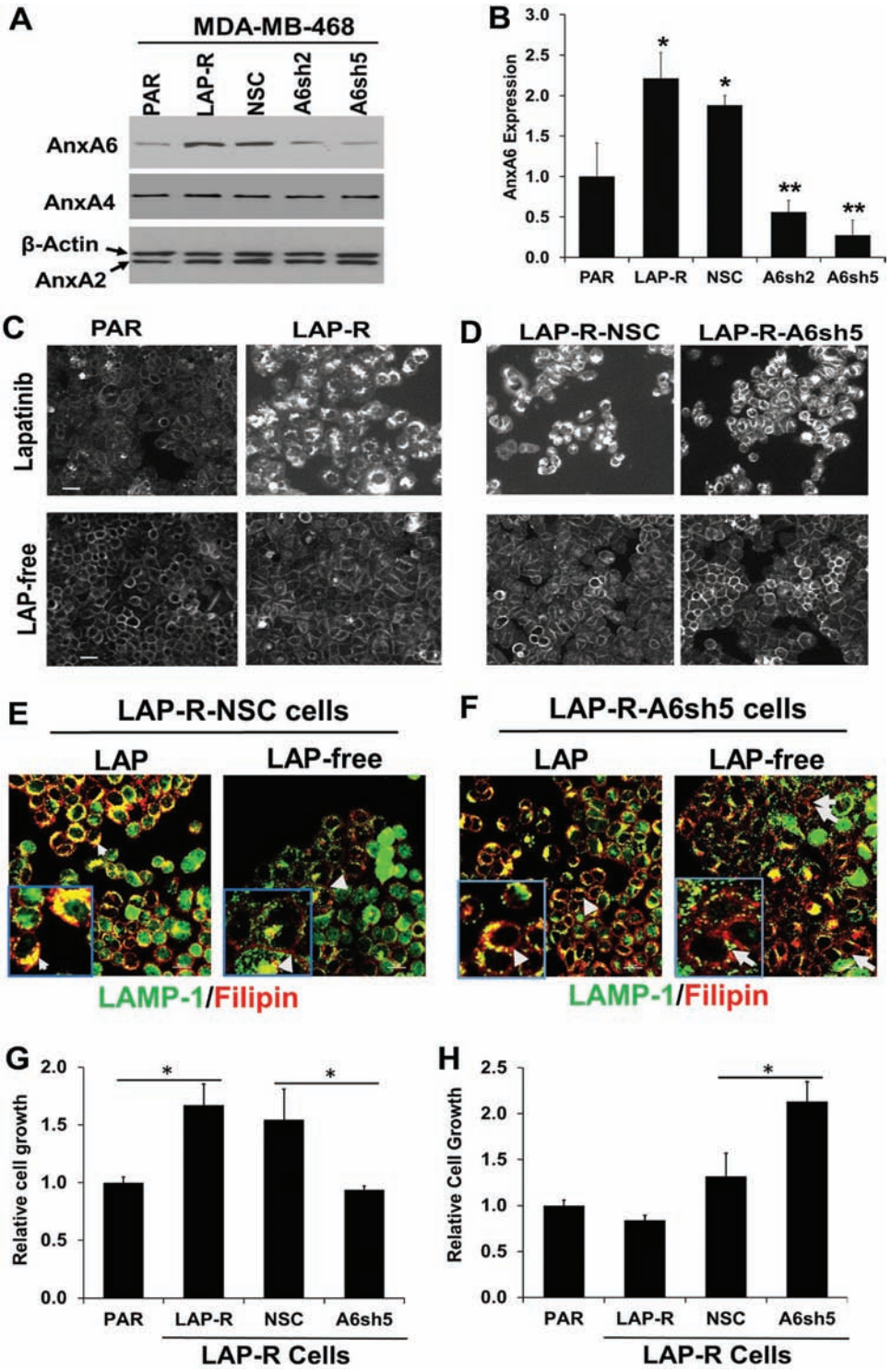

Figure 5. RNA interference mediated inhibition of lapatinib-induced AnxA6 upregulation in lapatinib-resistant cells blocked cholesterol accumulation in late endosomes and sensitized the cells to lapatinib. (**A**) The expression of AnxA6, AnxA4 and AnxA2 in lapatinib-treated cells was verified by western blotting using whole-cell lysates from MDA-MB-468 PAR, LAP-R or LAP-R cells transfected with control (26) and AnxA6-targeting shRNAs (A6sh2 and A6sh5). (**B**) Densitometric quantification of AnxA6 expression from three independent experiments. *$P < 0.05$ for LAP-R and NSC control versus PAR cells; **$P < 0.01$ for A6sh2 and A6sh5 cells versus NSC control cells. (**C** and **D**) Parental and LAP-R cells (C) or LAP-R-NSC and LAP-R-A6sh5 cells (D) were treated continuously with lapatinib or without lapatinib for 5 days and whole-cell cholesterol (filipin staining) was visualized by wide-field microscopy as described in Figure 3A. (**E** and **F**) LAP-R-NSC and LAP-R-A6sh5 cells cultured as described in Figure 3C were stained with LAMP-1 and filipin and visualized by confocal microscopy as in Figure 3B. (**G** and **H**) The indicated cell lines were continuously cultured in lapatinib containing medium (G) or without lapatinib (LAP free) for 5 days (H) and the viability of the cells assessed using the PrestoBlue cell viability assay reagent. *$P < 0.05$ for PAR versus LAP-R cells for lapatinib-treated cells versus NSC for LAP-free cells.

kinase pathway and that removal of lapatinib and enrichment of plasma membrane with cholesterol is associated with EGFR-dependent ERK1/2 activation.

Discussion

Despite the successful development of several TKIs and therapeutic monoclonal antibodies against the EGFR, their use in the management of TNBC, in particular, remains a major challenge due to the development of resistance against these drugs. Reliable biomarkers to monitor both the response to therapy and the ensuing resistance are still lacking. In this study, we demonstrate two additional previously undescribed effects of lapatinib and other EGFR-targeted TKIs in TNBC cells including upregulation of AnxA6 and accumulation of cholesterol in late endosomes. Our data reveal that lapatinib-induced expression of AnxA6 is critical in the development of resistance against this drug because prevention of AnxA6 upregulation by RNA interference not only inhibited cholesterol accumulation in late endosomes but also sensitized the cells to lapatinib. Interestingly, withdrawal of lapatinib not only restored AnxA6 expression to the basal levels but also relieved

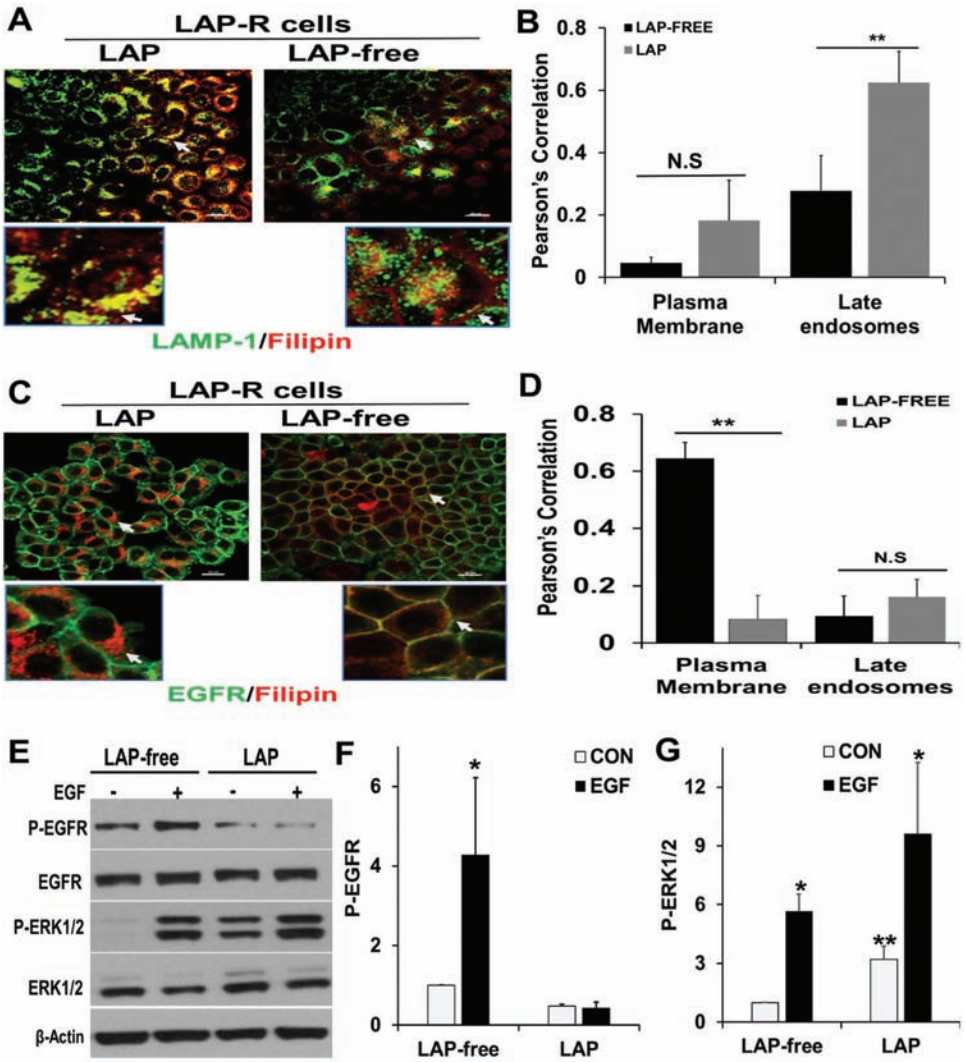

Figure 6. Withdrawal of lapatinib from lapatinib-resistant cells restored EGFR-dependent ERK1/2 activation. (**A**) LAP-R cells were grown on glass coverslips and processed as depicted in Figure 3C. Cells were washed, fixed in PBS-buffered 3.7% formaldehyde and stained with LAMP-1 and filipin as in Figure 3B. (**B**) Co-localization of residual cholesterol and LAMP-1 in the plasma membrane and late endosomes using the Nikon advanced research imaging software. Pearson's correlation denotes the extent of co-localization. $^{**}P = 0.02$ for co-localization of filipin and LAMP-1 ($n = 3$ cells). (**C**) Parental and LAP-R cells were treated continuously with lapatinib or without lapatinib as in Figure 3C, and whole-cell cholesterol (filipin staining) and EGFR were visualized by confocal microscopy as described in Figure 3B. (**D**) Co-localization of filipin and EGFR as assessed using Nikon advanced research imaging software. Pearson's correlation indicated the extent of co-localization of filipin and EGFR. $^{**}P = 0.01$ for co-localization of filipin and EGFR ($n = 3$ cells). N.S. denotes not significant. (**E**) LAP-R cells were maintained in lapatinib containing medium or in medium without lapatinib as in Figure 3C. Cells were then serum-starved overnight and stimulated with EGF for 5 min. Activation of EGFR and ERK1/2 were assessed by western blotting. Total ERK1/2 and EGFR as well as ACTB were used as loading controls. (**F** and **G**) Densitometric quantification of phospho-EGFR (F) and phospho-ERK1/2 (G). Bars represent activated EGFR or ERK1/2 relative to control from two independent experiments. $^{*}P < 0.05$ versus control (no EGF) and $^{**}P < 0.05$ for basal activation of ERK1/2 in LAP-free treatment versus continuous lapatinib treatment.

the lapatinib-induced accumulation of cholesterol, and led to cholesterol-enriched plasma membranes. This also restored the responsiveness of the cells to EGF and, consequently, activation of the MAP kinase ERK1/2. The increased AnxA6 expression and high cellular cholesterol have been independently reported to be associated with drug resistance. It is therefore plausible to suggest that the lapatinib-induced AnxA6 upregulation and accumulation of cholesterol constitute an adaptive mechanism for EGFR-expressing TNBC cells to overcome prolong treatment with EGFR-targeted TKIs.

Our finding that lapatinib induced the expression of AnxA6 protein and mRNA is consistent with previous studies showing that the expression of AnxA6 mRNA and/or protein is induced by exposure to radiation (39), the endocrine-disrupting chemical bisphenol A (40) and anti-cancer drugs such as the polypyrimidine, FdUMP (41). AnxA6 has also been shown to be differentially expressed during progression of osteoarthritis (42), uterine cervix carcinogenesis (43), progression of melanoma (44) and progression of HER-2/Neu oncogene-driven murine mammary tumors (45). In spite of this evidence, the molecular basis for lapatinib-induced AnxA6 expression remains unclear. Although other mechanisms are yet to be reported, ANXA6 promoter hypermethylation has been reported as a mechanism for its downregulation in gastric cancer (46) and perhaps other malignancies. It is possible that the rapid (transient drug treatment) and persistent (prolong drug treatment) upregulation of AnxA6 in lapatinib-treated cells may at least in part be due to lapatinib modulation of epigenetic pathways and may include hypomethylation of ANXA6 promoter.

The potential for AnxA6 as a biomarker for chronic diseases has been investigated in a number of studies. These include studies demonstrating that detection of AnxA6 may be useful to discriminate acute (AnxA6 low) from chronic (AnxA6 high) myocarditis (47), as a serum biomarker for esophageal adenocarcinoma (48), and to detect minimal residual disease in B-lineage acute lymphoblastic leukemia (49). Given that assays to reliably detect the development of resistance against EGFR-TKIs remain a major challenge, it seems probable that detection of AnxA6 along with cholesterol or other lipid raft markers before and after treatment with these drugs may be a reliable indicator of whether or not tumor cells can develop resistance to these drugs. However, further studies using a cohort of patients or mouse models of breast cancer treated with EGFR-targeted therapies are necessary to verify this possibility.

Our observation that lapatinib-induced upregulation of AnxA6 was accompanied by accumulation of cholesterol in late endosomes is consistent with other reports showing that overexpression of AnxA6 in the AnxA6-low Chinese hamster ovary cells led to localization of cholesterol in cytoplasmic or perinuclear vesicles (1,50). Although AnxA2 and AnxA4 were not affected by lapatinib treatment, AnxA2 has been shown to be associated with drug resistance in gastric cancer (51), whereas AnxA1 has been reported to be associated with resistance to Adriamycin in tumor cells (52). It is possible that distinct annexins mediate drug resistance via different mechanisms. In the case of AnxA6, this study suggests that accumulation and redistribution of cholesterol following prolong treatment of TNBC cells with EGFR-TKIs constitutes a major and presumably AnxA6-specific mechanism for acquired resistance. The increase in cholesterol in lapatinib-treated cells could be due to increased uptake by endocytosis and/or biosynthesis or diminished efflux due to inhibition of cholesterol transport proteins such as ABCA1. Regardless of the basis for the accumulation of cholesterol in lapatinib-treated cells, lapatinib-induced expression of AnxA6 appears to play a role in the retention of cholesterol and the associated acquired resistance. This is supported by the decrease in AnxA6 to basal levels following withdrawal of lapatinib. Our study underscores the need to target intracellular cholesterol (53), mitochondrial cholesterol (54), cholesterol uptake and disruption of membrane-associated cholesterol to sensitize cancer cells to diverse therapeutic regimens.

Perhaps the most important observations in this study are lapatinib-induced AnxA6 expression, accumulation of cholesterol and the increased basal EGFR-independent activation of ERK1/2. The association of cholesterol accumulation and activation of the MAP kinase ERK1/2 is consistent with a previous report showing that accumulation of cholesterol in late endosomes and lysosomes in Niemann-Pick type C1 (NPC1) disease promoted the activation of the MAP kinase signaling pathway (55). However, abundant evidence also suggests that inhibition of EGFR is associated with activation of other RTKs including MET and AXL (56,57) and, consequently, EGFR-independent activation of ERK1/2. As indicated earlier, withdrawal of lapatinib from LAP-R cells restored the cellular levels of AnxA6 to basal levels but, more importantly, led to a conspicuous association of AnxA6 with the plasma membrane. This suggests restoration of EGFR activity, the associated store-operated Ca^{2+} entry (SOCE) and, consequently, Ca^{2+}-dependent translocation of AnxA6 to the plasma membranes. This is supported by a recent report showing that RTK inhibitors inhibit Ca^{2+} influx including SOCE and that compared with erlotinib and gefitinib, lapatinib was the most effective inhibitor of SOCE (58). The strong inhibition of SOCE in lapatinib-treated cells is consistent with the more effective induction of AnxA6 expression observed in lapatinib-treated MDA-MB-468 cells compared with treatment with erlotinib or gefitinib. Because MDA-MB-468 cells actively synthesize EGFR, the enrichment of plasma membranes with cholesterol and Ca^{2+}-dependent membrane localization of AnxA6 strongly supports the restoration of EGFR-dependent activation of ERK1/2 following withdrawal of lapatinib. This is also supported by our previous study showing that AnxA6 stabilizes activated EGFR on the cell surface for persistent downstream signaling (25). In conclusion, we demonstrate that prolong lapatinib treatment induces resistance to the drug by induction of AnxA6 expression, accumulation of cholesterol in late endosomes, and EGFR-independent activation of ERK1/2. Although further studies are required to elucidate the mechanisms by which lapatinib and other TKIs induce AnxA6 expression in certain TNBC cells, the present study supports the option to target intracellular cholesterol rather than the current attempts at targeting EGFR and other RTKs, which does not prevent acquired resistance to the TKIs. This study also provides a strong rationale for further studies to validate the detection of AnxA6 along with cholesterol or other lipid raft markers as biomarkers for the detection of acquired resistance to lapatinib and other EGFR-TKIs.

Funding

National Institutes of Health (1SC1 CA211030, 5SC2 CA170244 to A.M.S.; U54MD007593, 5U54MD007586, U54CA163069, R24DA036420, S10RR0254970); NIH RISE (5R25GM059994 to S.E.W. and D.S.W.).

Author contributions

S.E.W. was responsible for the execution, data analyses and data interpretation, drafting of the manuscript and figures;

D.S.W. and O.Y.K. contributed in cell line maintenance, execution and data interpretation; J.S.G. helped with the microscopic analysis and data interpretation; J.O. and K.P.W. contributed to experimental design and editing of the manuscript; and A.M.S. designed the study and provided insight for experimental execution, the writing, reviewing and editing of the manuscript and figures. All authors have read and approved the final manuscript.

Acknowledgements

We thank Dr Brian B.Lehmann for the analysis of RNAseq data from the TBCRC001 clinical trial. We thank the directors and personnel in the Meharry Morphology Core facility for microscopy as well as Molecular Biology core facility for ultracentrifugation and other end point analysis.
Conflict of Interest Statement: None declared.

References

1. Badowska-Kozakiewicz, A.M. *et al.* (2016) Immunohistochemical characteristics of basal-like breast cancer. Contemp. Oncol. (Pozn)., 20, 436–443.
2. Cancer Genome Atlas Network (2012) Comprehensive molecular portraits of human breast tumours. Nature, 490, 61–70.
3. de Diego, I. *et al.* (2002) Cholesterol modulates the membrane binding and intracellular distribution of annexin 6. J. Biol. Chem., 277, 32187–32194.
4. Cheang, M.C. *et al.* (2008) Basal-like breast cancer defined by five biomarkers has superior prognostic value than triple-negative phenotype. Clin. Cancer Res., 14, 1368–1376.
5. Rakha, E.A. *et al.* (2009) Triple-negative breast cancer: distinguishing between basal and nonbasal subtypes. Clin. Cancer Res., 15, 2302–2310.
6. Tan, D.S. *et al.* (2008) Triple negative breast cancer: molecular profiling and prognostic impact in adjuvant anthracycline-treated patients. Breast Cancer Res. Treat., 111, 27–44.
7. Carey, L.A. *et al.* (2012) TBCRC 001: randomized phase II study of cetuximab in combination with carboplatin in stage IV triple-negative breast cancer. J. Clin. Oncol., 30, 2615–2623.
8. Ferraro, D.A. *et al.* (2013) Inhibition of triple-negative breast cancer models by combinations of antibodies to EGFR. Proc. Natl Acad. Sci. USA, 110, 1815–1820.
9. Arteaga, C. (2003) Targeting HER1/EGFR: a molecular approach to cancer therapy. Semin. Oncol., 30 (3 suppl. 7), 3–14.
10. Burness, M.L. *et al.* (2010) Epidermal growth factor receptor in triple-negative and basal-like breast cancer: promising clinical target or only a marker? Cancer J., 16, 23–32.
11. Redig, A.J. *et al.* (2013) Breast cancer as a systemic disease: a view of metastasis. J. Intern. Med., 274, 113–126.
12. Lambert, A.W. *et al.* (2017) Emerging biological principles of metastasis. Cell, 168, 670–691.
13. Liu, Q. *et al.* (2018) EGFR-TKIs resistance via EGFR-independent signaling pathways. Mol. Cancer, 17, 53.
14. Huang, L. *et al.* (2015) Mechanisms of resistance to EGFR tyrosine kinase inhibitors. Acta Pharm. Sin. B, 5, 390–401.
15. Irwin, M.E. *et al.* (2011) Lipid raft localization of EGFR alters the response of cancer cells to the EGFR tyrosine kinase inhibitor gefitinib. J. Cell. Physiol., 226, 2316–2328.
16. Zhang, Z. *et al.* (2016) Lipid raft localization of epidermal growth factor receptor alters matrix metalloproteinase-1 expression in SiHa cells via the MAPK/ERK signaling pathway. Oncol. Lett., 12, 4991–4998.
17. Pani, B. *et al.* (2009) Lipid rafts/caveolae as microdomains of calcium signaling. Cell Calcium, 45, 625–633.
18. Patra, S.K. *et al.* (2008) Molecular targets of (–)-epigallocatechin-3-gallate (EGCG): specificity and interaction with membrane lipid rafts. J. Physiol. Pharmacol., 59 (suppl. 9), 217–235.
19. Pommier, A.J. *et al.* (2010) Liver X receptor activation downregulates AKT survival signaling in lipid rafts and induces apoptosis of prostate cancer cells. Oncogene, 29, 2712–2723.
20. Li, Y.C. *et al.* (2006) Elevated levels of cholesterol-rich lipid rafts in cancer cells are correlated with apoptosis sensitivity induced by cholesterol-depleting agents. Am. J. Pathol., 168, 1107–1118; quiz 1404.
21. Mollinedo, F. *et al.* (2015) Lipid rafts as major platforms for signaling regulation in cancer. Adv. Biol. Regul., 57, 130–146.
22. Calder, P.C. *et al.* (2007) Lipid rafts–composition, characterization, and controversies. J. Nutr., 137, 545–547.
23. Rescher, U. *et al.* (2004) Annexins–unique membrane binding proteins with diverse functions. J. Cell Sci., 117, 2631–2639.
24. Qi, H. *et al.* (2015) Role of annexin A6 in cancer. Oncol. Lett., 10, 1947–1952.
25. Koumangoye, R.B. *et al.* (2013) Reduced annexin A6 expression promotes the degradation of activated epidermal growth factor receptor and sensitizes invasive breast cancer cells to EGFR-targeted tyrosine kinase inhibitors. Mol. Cancer, 12, 167.
26. Spigel, D.R. *et al.* (2013) Randomized phase II trial of onartuzumab in combination with erlotinib in patients with advanced non-small-cell lung cancer. J. Clin. Oncol., 31, 4105–4114.
27. Goodwin, J.S. *et al.* (2005) Ras diffusion is sensitive to plasma membrane viscosity. Biophys. J., 89, 1398–1410.
28. Macdonald, J.L. *et al.* (2005) A simplified method for the preparation of detergent-free lipid rafts. J. Lipid Res., 46, 1061–1067.
29. Franken, N.A. *et al.* (2006) Clonogenic assay of cells *in vitro*. Nat. Protoc., 1, 2315–2319.
30. Thompson, P.D. *et al.* (2014) Alpha-2 Heremans Schmid glycoprotein (AHSG) modulates signaling pathways in head and neck squamous cell carcinoma cell line SQ20B. Exp. Cell Res., 321, 123–132.
31. Hudachek, S.F. *et al.* (2013) Physiologically based pharmacokinetic model of lapatinib developed in mice and scaled to humans. J. Pharmacokinet. Pharmacodyn., 40, 157–176.
32. Kim, R. *et al.* (2001) Pharmacokinetic and biochemical analysis in the treatment of weekly paclitaxel in relapsed breast cancer. Oncol. Rep., 8, 1171–1176.
33. Go, R.S. *et al.* (1999) Review of the comparative pharmacology and clinical activity of cisplatin and carboplatin. J. Clin. Oncol., 17, 409–422.
34. Liedtke, C. *et al.* (2008) Response to neoadjuvant therapy and long-term survival in patients with triple-negative breast cancer. J. Clin. Oncol., 26, 1275–1281.
35. Sakwe, A.M. *et al.* (2011) Annexin A6 contributes to the invasiveness of breast carcinoma cells by influencing the organization and localization of functional focal adhesions. Exp. Cell Res., 317, 823–837.
36. Freeman, M.R. *et al.* (2004) Cholesterol and prostate cancer. J. Cell. Biochem., 91, 54–69.
37. Rajamanickam, G.D. *et al.* (2017) Na/K-ATPase regulates bovine sperm capacitation through raft- and non-raft-mediated signaling mechanisms. Mol. Reprod. Dev., 84, 1168–1182.
38. Yang, P. *et al.* (2014) Cellular location and expression of Na+, K+-ATPase α subunits affect the anti-proliferative activity of oleandrin. Mol. Carcinog., 53, 253–263.
39. Turtoi, A. *et al.* (2010) Proteomic and genomic modulations induced by γ-irradiation of human blood lymphocytes. Int. J. Radiat. Biol., 86, 888–904.
40. Lee, H.S. *et al.* (2018) Proteomic biomarkers for bisphenol A–early exposure and women's thyroid cancer. Cancer Res. Treat., 50, 111–117.
41. Gmeiner, W.H. *et al.* (2010) Genome-wide mRNA and microRNA profiling of the NCI 60 cell-line screen and comparison of FdUMP[10] with fluorouracil, floxuridine, and topoisomerase 1 poisons. Mol. Cancer Ther., 9, 3105–3114.
42. Pfander, D. *et al.* (2001) Expression of early and late differentiation markers (proliferating cell nuclear antigen, syndecan-3, annexin VI, and alkaline phosphatase) by human osteoarthritic chondrocytes. Am. J. Pathol., 159, 1777–1783.
43. Lomnytska, M.I. *et al.* (2011) Differential expression of ANXA6, HSP27, PRDX2, NCF2, and TPM4 during uterine cervix carcinogenesis: diagnostic and prognostic value. Br. J. Cancer, 104, 110–119.
44. Francia, G. *et al.* (1996) Identification by differential display of annexin-VI, a gene differentially expressed during melanoma progression. Cancer Res., 56, 3855–3858.
45. Croci, S. *et al.* (2010) Proteomic and PROTEOMEX profiling of mammary cancer progression in a HER-2/neu oncogene-driven animal model system. Proteomics, 10, 3835–3853.

46. Wang, X. *et al.* (2013) Annexin A6 is down-regulated through promoter methylation in gastric cancer. Am. J. Transl. Res., 5, 555–562.
47. Bian, Z. *et al.* (2009) Change of cardiac function in experimental autoimmune myocarditis is correlated with the expression of annexin VI. Acta Cardiol., 64, 71–77.
48. Zaidi, A.H. *et al.* (2014) Evaluation of a 4-protein serum biomarker panel-biglycan, annexin-A6, myeloperoxidase, and protein S100-A9 (B-AMP)-for the detection of esophageal adenocarcinoma. Cancer, 120, 3902–3913.
49. Chen, X. *et al.* (2001) Quantification of minimal residual disease in T-lineage acute lymphoblastic leukemia with the TAL-1 deletion using a standardized real-time PCR assay. Leukemia, 15, 166–170.
50. Cubells, L. *et al.* (2007) Annexin A6-induced alterations in cholesterol transport and caveolin export from the Golgi complex. Traffic, 8, 1568–1589.
51. Zhang, Z.D. *et al.* (2014) Annexin A2 is implicated in multi-drug-resistance in gastric cancer through p38MAPK and AKT pathway. Neoplasma, 61, 627–637.
52. Bai, X.F. *et al.* (2004) Overexpression of annexin 1 in pancreatic cancer and its clinical significance. World J. Gastroenterol., 10, 1466–1470.
53. Mandal, C.C. *et al.* (2014) Targeting intracellular cholesterol is a novel therapeutic strategy for cancer treatment. J. Cancer Sci. Ther., 6, 510–513.
54. Montero, J. *et al.* (2008) Mitochondrial cholesterol contributes to chemotherapy resistance in hepatocellular carcinoma. Cancer Res., 68, 5246–5256.
55. Sawamura, N. *et al.* (2001) Site-specific phosphorylation of tau accompanied by activation of mitogen-activated protein kinase (MAPK) in brains of Niemann-Pick type C mice. J. Biol. Chem., 276, 10314–10319.
56. Linklater, E.S. *et al.* (2016) Targeting MET and EGFR crosstalk signaling in triple-negative breast cancers. Oncotarget, 7, 69903–69915.
57. Scaltriti, M. *et al.* (2016) Molecular pathways: AXL, a membrane receptor mediator of resistance to therapy. Clin. Cancer Res., 22, 1313–1317.
58. Emeriau, N. *et al.* (2018) Store operated calcium entry is altered by the inhibition of receptors tyrosine kinase. Oncotarget, 9, 16059–16073.